FULL PAPER

# Factors Governing Intercalation of Fullerenes and Other Small Molecules Between the Side Chains of Semiconducting Polymers Used in Solar Cells

*Nichole Cates Miller, Eunkyung Cho, Roman Gysel, Chad Risko, Veaceslav Coropceanu, Chad E. Miller, Sean Sweetnam, Alan Sellinger, Martin Heeney, Iain McCulloch, Jean-Luc Brédas, Michael F. Toney, and Michael D. McGehee**

**While recent reports have established significant miscibility in polymer:fullerene blends used in organic solar cells, little is actually known about why polymers and fullerenes mix and how their mixing can be controlled. Here, X-ray diffraction (XRD), differential scanning calorimetry (DSC), and molecular simulations are used to study mixing in a variety of polymer:molecule blends by systematically varying the polymer and small-molecule properties. It is found that a variety of polymer:fullerene blends mix by forming bimolecular crystals provided there is sufficient space between the polymer side chains to accommodate a fullerene. Polymer:tetrafluoro-tetracyanoquinodimethane (F4-TCNQ) bimolecular crystals were also observed, although bimolecular crystals did not form in the other studied polymer:non-fullerene blends, including those with both conjugated and non-conjugated small molecules. DSC and molecular simulations demonstrate that strong polymer–fullerene interactions can exist, and the calculations point to van der Waals interactions as a significant driving force for molecular mixing.**

N. C. Miller, Dr. R. Gysel, Dr. C. E. Miller, S. Sweetnam, Dr. A. Sellinger, Prof. M. D. McGehee
Department of Materials Science and Engineering
Stanford University, Stanford, CA 94305, USA
E-mail: mmcghehee@stanford.edu
E. Cho, Dr. C. Risko, Dr. V. Coropceanu, Prof. J.-L. Brédas
School of Chemistry & Biochemistry
and Center for Organic Photonics and Electronics
Georgia Institute of Technology
Atlanta, GA 30332, USA
E. Cho
School of Materials Science and Engineering
Georgia Institute of Technology
Atlanta, GA 30332, USA
Dr. M. F. Toney
Stanford Synchrotron Radiation Lightsource
SLAC National Accelerator Laboratory
Menlo Park, CA 94025, USA
Prof. M. Heeney, Prof. Iain McCulloch
Department of Chemistry
Imperial College London
London SW7 2AZ, UK

**DOI: 10.1002/aenm.201200392**

## 1. Introduction

Bulk heterojunction organic solar cells based on blends of a conjugated polymer (donor) and a fullerene derivative (acceptor) have attracted considerable attention due to their rapidly increasing efficiencies and their potential as a low-cost, printable, and flexible renewable energy source.[1–3] Until recently, polymer:fullerene blends were thought to phase separate into pure polymer and pure fullerene domains. However, recent studies using a variety of techniques – including small-angle neutron scattering (SANS),[4,5] scanning transmission X-ray microscopy (STXM),[6] dynamic secondary ion mass spectrometry (DSIMS),[5–7] energy-filtered transmission electron microscopy (EFTEM),[8,9] photoluminescence,[10–15] and X-ray scattering[8,12–16]– have altered this traditional view. For instance, studies of blends of the semi-crystalline polymer poly(3-hexylthiophene) (P3HT) with the fullerene derivative phenyl-$C_{61}$-butyric acid methyl ester (PCBM-C60) have demonstrated the existence of pure crystalline P3HT, pure PCBM-C60, and molecularly mixed, amorphous P3HT:PCBM-C60 domains.[4–9] Furthermore, molecular mixing has been demonstrated in amorphous MDMO-PPV:PCBM-C60 blends.[11,17–19] Polymer:fullerene molecular mixing can also occur in semicrystalline domains via fullerene intercalation between the polymer side chains to form polymer:fullerene bimolecular crystals (**Figure 1**).[12–16,20–22]

The concept of intermixed donor–acceptor interfaces, which exist in intercalated polymer:fullerene blends as well as molecularly mixed amorphous blends, challenges to some extent the notions regarding the operation of organic solar cells, as it is generally hypothesized that excitons originating in a pure phase diffuse to a polymer–fullerene (donor–acceptor) interface and split into separated charges (that are then extracted from the device via migration through the pure phases). That intermixing occurs in many polymer:fullerene blends should impact solar-cell operation, as the very nature of the donor–acceptor interface changes. For example, molecular mixing due to intercalation in semicrystalline blends or miscibility in amorphous

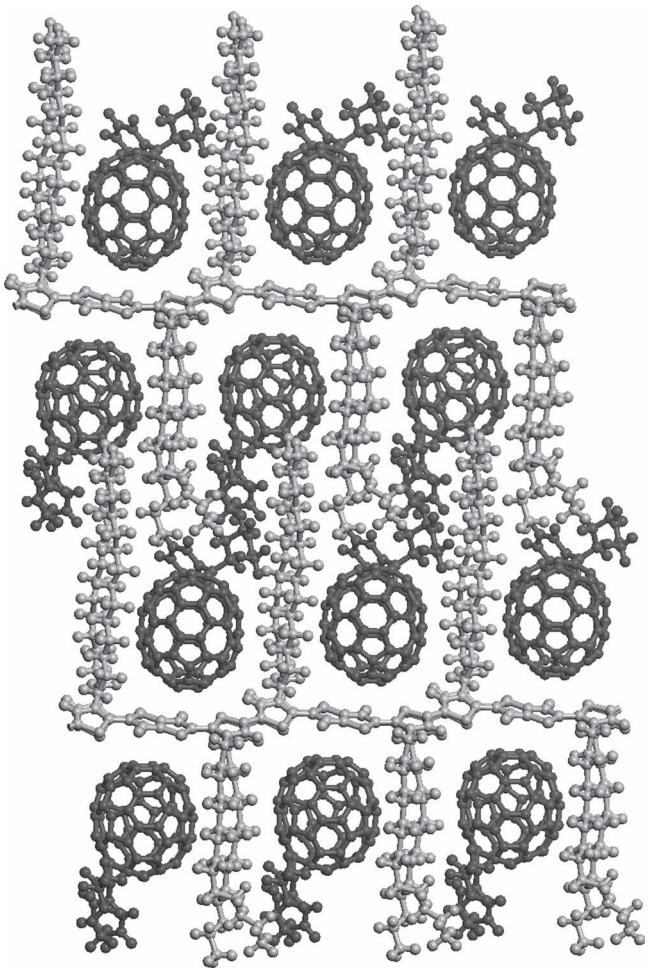

**Figure 1.** Fullerene intercalation between the polymer side chains in the PBTTT-C14:PCBM-C70 bimolecular crystal. The PBTTT polymer and PCBM-C70 fullerene are light and dark gray, respectively.

blends can improve exciton splitting, since excitons originating in molecularly mixed domains form within a few angstroms of a donor-acceptor interface.[4,10–15] Thus, exciton splitting in molecularly mixed domains does not require exciton diffusion on the 5–10 nm length scale.[23] However, the intimate mixing of the donor and acceptor in molecularly mixed blends can also introduce (polaron) traps that can foster larger recombination rates versus those observed for completely separate donor and acceptor phases.[15,16] In addition, molecular mixing alters the minimum fullerene content needed for the formation of pure fullerene domains, which appear to be required for good electron transport, and consequently affects the polymer:fullerene ratio required for peak solar-cell performance.[12,13] Other important properties such as optical absorption[12–15] and fracture energy[24] can also be affected by molecular mixing. It is therefore necessary to understand molecular mixing to properly describe the electronic processes in polymer:fullerene blends and rationally design more efficient solar cells, since molecular mixing, for instance that due to intercalation, has been shown to significantly impact many solar-cell properties.

Still, there are many unanswered questions regarding molecular mixing. For instance, how do the size, conjugation, and electron-accepting properties of small molecules affect how they mix with polymers? Does molecular mixing occur in all polymer:fullerene blends? And what polymer–fullerene interactions are responsible for molecular mixing? Here, we use X-ray diffraction (XRD), differential scanning calorimetry (DSC), and molecular simulations to explore these and other questions. Our target systems are those distinctive cases of bimolecular-crystal formation through fullerene (and other small molecule) intercalation between the polymer side chains. We do this by systematically varying the polymer, fullerene, and small-molecule properties to determine their effect on intercalation.

In agreement with previous results,[12,13] we find that increasing the fullerene size through the addition of multiple bulky side groups can sterically prevent fullerene intercalation. We also show that intercalation can be inhibited by decreasing the space available between the polymer side chains either by decreasing the side-chain repeat distance or by replacing linear side chains with bulkier, branched side chains. Although many polymer:fullerene blends form intercalated bimolecular crystals, only one of the studied non-fullerene small molecules formed polymer:small molecular bimolecular crystals – tetrafluoro-tetracyanoquinodimethane (F4-TCNQ). We also probe the strength of the polymer–fullerene interaction responsible for intercalation by measuring the enthalpies of melting of the polymer:fullerene blends and their pure components using DSC and by evaluating the interaction (binding) energy of two bimolecular crystals and their pure components using molecular simulations.

## 2. Results & Discussion

### 2.1. PBTTT Blends with Fullerenes

We began by using specular XRD and 2D grazing incidence X-ray scattering (2D GIXS) to study intercalation in poly-(2,5-bis(3- tetradecylthiophene-2-yl)thieno[3,2-b]thiophene) (PBTTT-C14):fullerene blends. We chose PBTTT-C14 as the conjugated polymer due to its high crystallinity, which facilitates structure determination using XRD.[25] **Figure 2** shows the to-scale chemical structures of the 13 studied fullerenes as well as the lamellar spacing and lamellar-spacing increase relative to pure PBTTT-C14 for each blend. The lamellar spacings of pure PBTTT-C14 and PBTTT-C14:PCBM-C60 are 21.5 Å and 31.0 Å, respectively. All XRD patterns can be viewed in the Supporting Information.

A wide variety of fullerene derivatives form bimolecular crystals with PBTTT-C14. For instance, PCBM based on the C60,[12,15] C70,[12,13] and C84 fullerene cages all intercalate in PBTTT-C14. As expected, the lamellar spacings of the PBTTT:PCBM films approximately scale with the size of the fullerene cages. LuPCBEH-C80,[26] an endohedral fullerene containing three lutetium atoms, also intercalates in PBTTT-C14. These results indicate that slight changes to the size and nature of the fullerene cages do not prevent intercalation.

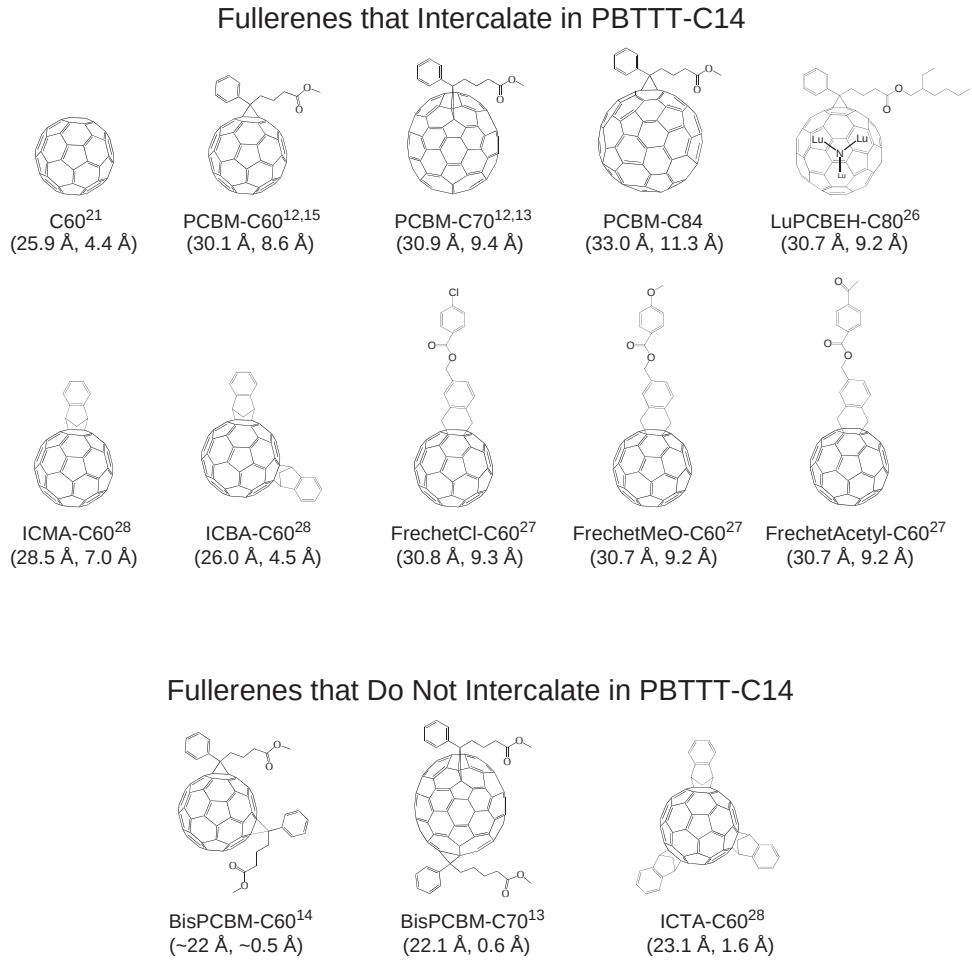


**Figure 2.** Chemical structures of the fullerenes tested for intercalation in PBTTT-C14. The numbers in parentheses are the lamellar spacings of the PBTTT-C14:fullerene blends and the lamellar spacings of the blends relative to pure PBTTT-C14, respectively.

The fullerene side groups were also varied to determine their effect on bimolecular-crystal formation. Fullerenes with large side groups (the dihydronaphthyl-bridged ester fullerene derivatives FrechetCl-C60, FrechetMeO-C60, and FrechetAcetyl-C60),[27] small side groups (PCBM-C60,[12,15] PCBM-C70,[12,13] PCBM-C84, ICMA-C60,[28] and ICBA-C60[28]), and even no side groups (C60[21]) are able to intercalate in PBTTT-C14. The fact that fullerene side groups are not necessary for intercalation to occur suggests that the interaction between the fullerene cage and the polymer is a critical contributor to intercalation.

Furthermore, from earlier results, it is known that the interaction between the fullerene cage and the polymer backbone must be strong. We previously used a combination of XRD techniques, solid-state nuclear magnetic resonance (NMR) spectroscopy, and molecular mechanics simulations to determine the molecular packing in the intercalated PBTTT-C14:PCBM-C70 bimolecular crystal.[21] We found that the pi-stacking of pure PBTTT-C14 is significantly disrupted by the intercalation of PCBM-C70 and that each polymer backbone twists toward the closest PCBM-C70. These results indicate that the polymer–fullerene interaction in the PBTTT-C14:PCBM-C70 blend is very significant indeed.

Of the 13 fullerenes tested for intercalation in PBTTT-C14, only three do not intercalate: BisPCBM-C60,[14] BisPCBM-C70,[13] and ICTA-C60.[28] For these fullerenes, the lamellar spacing of the pure polymer is very close to that of the polymer:fullerene blend, indicating that the addition of the fullerene does not significantly change the packing of the polymer. Small increases in the lamellar spacing may be due to increased disorder in the film upon the addition of the fullerene. That these fullerenes do not intercalate is not surprising given that the bulkiness of these molecules does not allow them to fit between the PBTTT-C14 side chains. The fact that ICBA intercalates even though BisPCBM-C60 and BisPCBM-C70 do not is likely due to the less bulky indene side groups on ICBA-C60 relative to the side groups of BisPCBM-C60 and BisPCBM-C70.[28]

The lamellar spacings of the intercalated PBTTT-C14:fullerene blends are smaller than those estimated from the simple addition of the fullerene size to the lamellar spacing of pure PBTTT-C14. For example, although the outer diameter of C60 is ~10 Å,[29] the lamellar-spacing increase of PBTTT-C14:C60 relative to pure PBTTT-C14 is only 4.4 Å. The other intercalated PBTTT-C14:fullerene blends also exhibit this smaller-than-expected increase in lamellar spacing. While differences in the tilt angle

and the amount of disorder in the polymer side chains in pure PBTTT-C14 and PBTTT-C14:fullerene blends may account for this difference, it should be noted that the side chains in pure PBTTT are only partially interdigitated, with ~4–5 of the methylene units in a non-interdigitated region as illustrated in Figure S6.[30] Thus, fullerenes that intercalate close to the polymer backbones actually occupy some previously unfilled space. This may explain why the density of the PBTTT-C14:PCBM-C70 blend was found to be higher than that of pure PBTTT-C14.[21]

It is also interesting to note that the lamellar spacings of the PBTTT-C14 blends with FrechetCl-C60, FrechetMeO-C60, and FrechetAcetyl-C60 fullerenes, which have very large side groups, are not much larger than the lamellar spacing of the PBTTT-C14:PCBM-C60 blend, likely because these large side groups are quite flexible and can fold back on themselves (vs. being fully extended). The unexpectedly small lamellar spacing of PBTTT-C14:ICBA-C60 blends, which has been discussed in detail in a recent work,[28] is due to the orientation of the two ICBA-C60 side groups perpendicular to the PBTTT-C14 side chains such that the ICBA-C60 side groups do not contribute to the lamellar spacing of the bimolecular crystal.

### 2.2. PBTTT Blends with Non-Conjugated Small Molecules

We next discuss intercalation in PBTTT-C14 blends with a variety of non-conjugated small molecules, many of which were chosen for their cage-like structures that mimic the shape and size of fullerenes. The studied molecules include several diamondoids, Kelevan, and two silsesquioxane derivatives, OVS and SSQ-Es (**Figure 3**). None of the non-conjugated molecules investigated intercalate in PBTTT-C14. We suspect that the high tendency of the diamondoids adamantane and triamantane and un-substituted OVS to crystallize could be partially responsible for these molecules not intercalating in PBTTT-C14, since they would rather crystallize with themselves than form bimolecular crystals (see molecular simulations below). Methylated triamantane and OH-diamantane were therefore studied due to their lower tendency to crystallize, but neither of these intercalated in PBTTT-C14. Finally the mono-substituted SSQ-Es was synthesized in an effort to mimic the size and methyl ester component of PCBM. However, no intercalation was observed for SSQ-Es. These results suggest that π-conjugation is an important factor for intercalation to occur, since it can allow stronger interactions between the polymer backbone and the intercalated molecule (*i.e.*, van der Waals, electrostatic, or charge-transfer interactions), for instance due to the higher polarizability of the electron cloud.

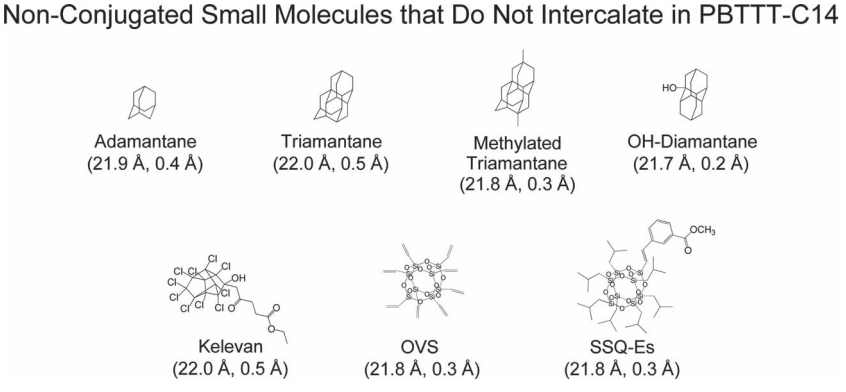


**Figure 3.** Chemical structures of the non-conjugated small molecules tested for intercalation in PBTTT-C14. None of these molecules intercalated in PBTTT-C14. The numbers in parentheses are the lamellar spacings of the PBTTT-C14:fullerene blends and the lamellar spacings of the blends relative to pure PBTTT-C14, respectively.

### 2.3. PBTTT Blends with Conjugated Small Molecules

The five non-fullerene, conjugated small molecules shown in **Figure 4** were tested for intercalation in PBTTT-C14 to look for non-fullerene molecules that intercalate in PBTTT-C14. Coronene and pyrene were chosen due to their fused aromatic ring structures that are similar to portions of fullerenes. These molecules, which are not typical electron acceptors, are found not to intercalate in PBTTT-C14. Two small-molecule acceptors, tetracyanoquinodimethane (TCNQ) and the vinazene derivative V-BT (that has been used successfully as a fullerene replacement in organic photovoltaics),[31,32] also did not intercalate in PBTTT-C14. Although the large size of V-BT could prevent intercalation, it is less clear why TCNQ does not intercalate since it is both conjugated and an electron acceptor. We can therefore conclude that factors other than conjugation and electron-acceptor character impact the ability of a molecule to intercalate in PBTTT-C14.

Of the non-fullerene small molecules we studied, F4-TCNQ was the only one to intercalate in PBTTT-C14. Because F4-TCNQ forms ground-state charge-transfer complexes with thiophene polymers[33] and thiophene small molecules,[34,35] it is expected that it can also form a ground-state charge-transfer complex with PBTTT-C14. Ground-state charge-transfer complexes form due to the partial or full transfer of an electron from the donor to the acceptor in the ground state, and thus give rise to material properties that are associated with neither the donor nor the acceptor (i.e., new absorption bands).[36–39] Note that ground-state charge-transfer complexes are different than the excited charge-transfer states of conventional donor-acceptor complexes that can be populated either by a photo-induced electron transfer (involving either a donor or an acceptor excited state) or via a direct excitation from the system ground state.[40] The formation of a PBTTT-C14:F4-TNCQ charge-transfer complex can be understood from the fact that the F4-TCNQ electron affinity (5.2 eV) is larger than the PBTTT-C14 ionization potential (5.1 eV).[33,41]

### 2.4. Other Semi-Crystalline Polymers

Polymer:fullerene bimolecular crystals will be sterically prevented from forming if there is not enough space between the polymer side chains to accommodate a fullerene.[12,13] Thus, it is important to consider the fullerene

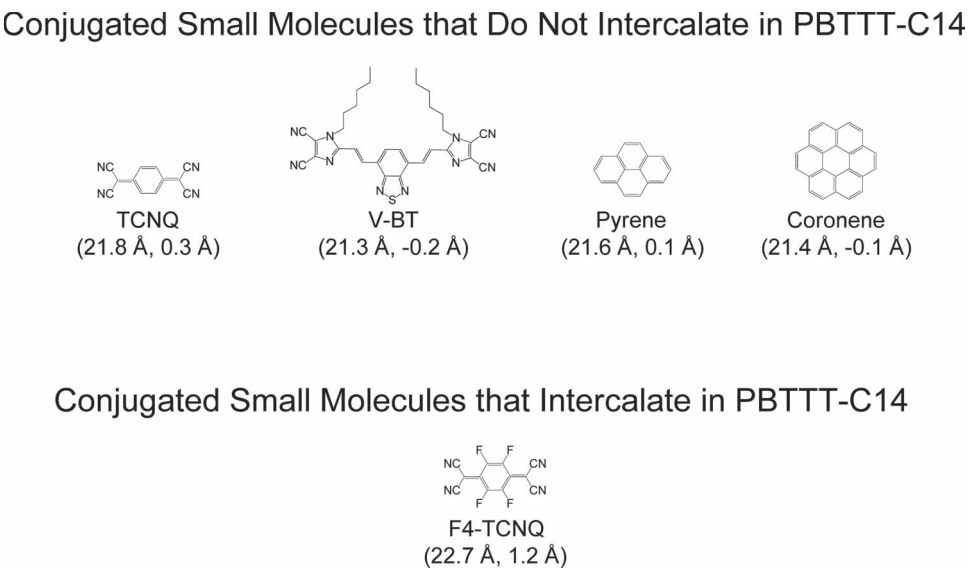


**Figure 4.** Chemical structures of the conjugated small molecules tested for intercalation in PBTTT-C14. The numbers in parentheses are the lamellar spacings of the PBTTT-C14:fullerene blends and the lamellar spacings of the blends relative to pure PBTTT-C14, respectively.

size relative to the space available between the polymer side chains when predicting if intercalation will occur. As discussed above, intercalation can be prevented by increasing the size of the fullerene derivative. We now show that intercalation can also be inhibited by decreasing the space between the polymer side chains, either by decreasing the side-chain attachment spacing or by replacing linear side chains with bulkier, branched side chains.

**Figure 5** shows the polymers tested for fullerene intercalation. To assess the generality of our previous observations, we used specular XRD to determine if intercalation occurs in poly(5,5 -bis(3-alkyl-2-thienyl)-2,2–bithiophene) (PQT) blends with PCBM-C60,[12] PCBM-C70, BisPCBM-C70, OVS, SSQ-Es, adamantane, triamantane, and Kelevan. The only difference between PBTTT-C12 and PQT is that the fused thienothiophene ring in PBTTT-C12 is replaced with two separate thiophene rings in PQT. For all PQT blends studied, the molecules that intercalate in PBTTT-C14 also intercalate in PQT, and the molecules that do not intercalate in PBTTT-C14 also do not intercalate in PQT. The same holds true for blends with PBTTT-C12 and PBTTT-C16. These results demonstrate that the differences between the PBTTT and PQT polymer backbones and changes to the PBTTT side-chain length do not affect if intercalation occurs.

PCBM intercalation also occurs in many other conjugated polymers. For instance, Siebbeles and Deibel used XRD and photoluminescence quenching measurements to demonstrate that PCBM forms bimolecular crystals with poly(2,5-bis(3-dodecylthiophen-2-yl)thieno[2,3-b]thiophene) (PBTCT).[15,16] PBTCT is similar to PBTTT-C12 except for the isomeric thieno[2,3-b]thiophene. XRD has also been used to demonstrate PCBM intercalation in the poly(terthiophene) polymer PTT.[12,42] Furthermore, Kim and co-workers[43] have shown that PCBM most likely intercalates in poly(3-(4-n-octyl) phenyl-5,2 ,5',2''-terthiophene) (POPTT) and poly(3-(4-n-octyl) phenyl-5,2′,5′,2″,5″,2‴-quaterthiophene) (POPQT), two polymers that are similar to PTT, since both POPTT and POPQT have sufficient space between their side chains to accommodate a fullerene and exhibit their highest solar-cell efficiencies at a 1:3 polymer:fullerene ratio. On the other hand, they show that the similar polymer poly(3-(4-n-octyl)phenylthiophene) (POPT), which is comparable to P3HT but with bulkier side chains, probably does not exhibit fullerene intercalation, because it has a short side-chain attachment distance and exhibits its highest efficiencies at a 1:1 polymer:fullerene ratio. Likewise, PCBM cannot intercalate in crystalline P3HT due to its small side-chain attachment spacing,[12] although intimate polymer:fullerene molecular mixing does occur in amorphous P3HT domains.[4–9]

The replacement of linear polymer side chains with branched side chains can also inhibit intercalation due to the decreased space available between the polymer side chains for fullerene intercalation. Specular XRD and 2D GIXS were used to demonstrate that intercalation does not occur in PBTTT when its linear side chains are replaced by lightly branched 3,7-dimethyloctyl side chains. Likewise, Heiser recently reported that branched side chains appear to inhibit intercalation in PTBzT$^2$ blends (based on optimization of power conversion efficiencies).[44] PTBzT$^2$-β is identical to PBTTT-C12 except for the addition of a benzothiadiazole group between the two unfused thiophene rings, so it is not surprising for fullerene intercalation to occur in PTBzT$^2$-α and PTBzT$^2$-β.The fact that branched side chains appear to inhibit intercalation in both PBTTT and PTBzT$^2$ may have implications for the highest performing polymers, since many of them contain branched side chains.[45–50] Still, it remains unclear how side-chain branching affects molecular mixing in amorphous domains.

Our results indicate that intercalation can only occur in crystalline domains if there is enough space between the polymer side chains to accommodate a fullerene. However, this does

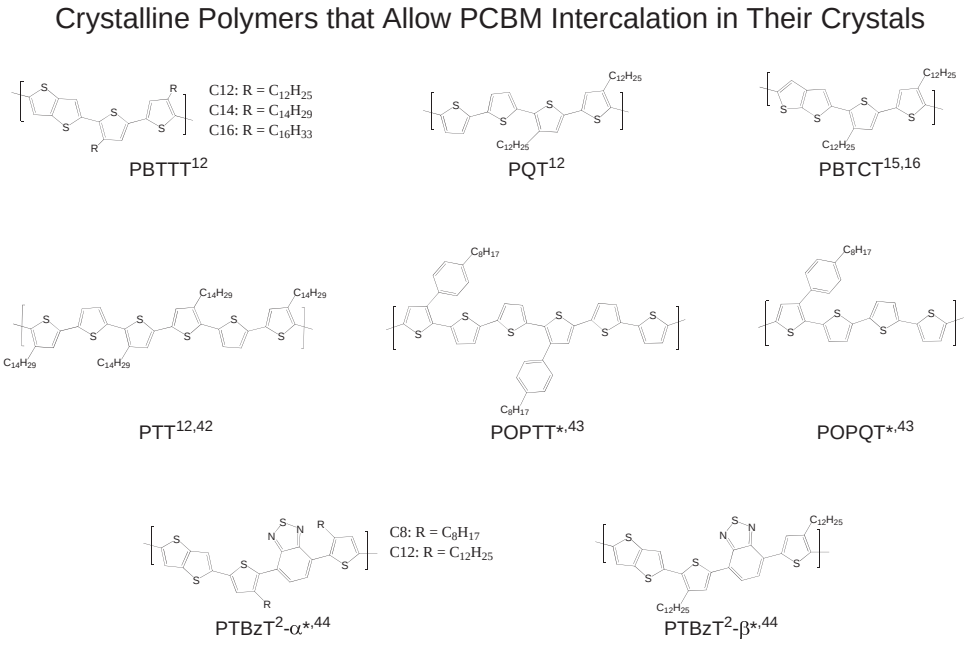


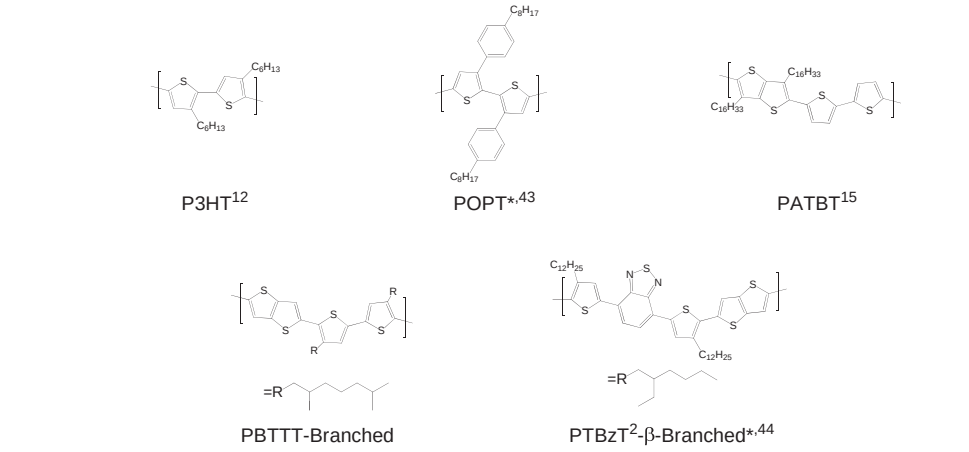


**Figure 5.** Chemical structures of the semi-crystalline polymers studied for PCBM intercalation. *Based on efficiency vs. polymer:fullerene ratio data and/or measurements of phase separation rather than XRD data.

not imply that all polymers that can accommodate a fullerene between its side chains will form polymer:fullerene bimolecular crystals. For example, specular XRD measurements have shown that PCBM-C60 does not intercalate in the semiconducting polymer poly(3,6-dialkylthieno[3,2-*b*]thiophene-*co*-bithiophene) (PATBT) despite the fact that the side-chain repeat distance of PATBT is exactly the same as that of PBTTT.[15] In fact, the only difference between PATBT and PBTTT-C16 is that the side chains attach to the thienothiophene ring in PATBT, while they attach to the unfused thiophene rings in PBTTT-C16. While it remains unclear why PCBM-C60 intercalates in PBTTT and not in PATBT, this difference is probably not due to the fact that PCBM-C60 would interact with unfused bi-thiophene units if it were to intercalate in PATBT (as opposed to the interaction of PCBM with the thienothiophene units in PBTTT), because PCBM-C60 also intercalates in PQT, which only has unfused bi-thiophene units. We suggest that differences in the planarity of the polymer backbones or the ability of the PBTTT side chains

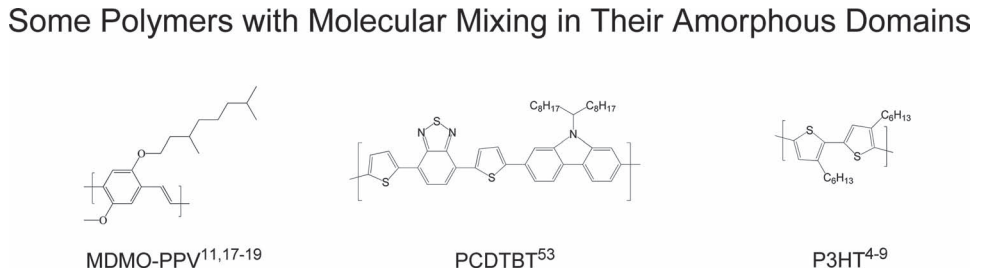


**Figure 6.** Chemical structures of some polymers with polymer:fullerene molecular mixing in their amorphous domains.

to move independently in contrast to the correlated movement of the PATBT side chains, which are attached to the same thienothiophene unit, could contribute to this difference.[51]

### 2.5. Amorphous Polymers and Semi-Crystalline Polymers with Low Crystallinity

Thus far, we have only discussed intercalation in crystalline domains that can be easily studied with XRD techniques. However, there is a significant amount of evidence for molecular mixing that involves intermixing in amorphous polymer:fullerene blends and in the amorphous domains of semi-crystalline polymer:fullerene blends (i.e., P3HT:PCBM blends).[4–9] **Figure 6** shows some of the polymers for which polymer:fullerene miscibility has been demonstrated in amorphous domains. For instance, we previously used a combination of photoluminescence measurements, scanning electron microscopy, and space-charge limited current measurements to demonstrate molecular mixing in poly(2-methoxy-5-(3′-7′-dimethyloctyloxy)-1,4-phenylenevinylene) (MDMO-PPV):PCBM blends.[11] Grey et al. subsequently used Raman spectroscopy to show specific changes in the vinylene groups of MDMO-PPV when it is blended with PCBM-C60.[52] This result could indicate a preferential interaction of PCBM-C60 with the vinylene groups in MDMO-PPV; such a preferred polymer–fullerene interaction could indicate intercalation of the PCBM-C60 between the MDMO-PPV side chains rather than a randomly dispersed mixture of MDMO-PPV and PCBM-C60. Measurements of photoluminescence and phase separation also indicate molecular mixing in PCDTBT:PCBM blends.[53] The ability to measure and understand molecular mixing in amorphous polymer:fullerene blends will become increasingly important since many of the new, high efficiency polymer:fullerene blends are either amorphous or are poorly crystalline.[53,54]

### 2.6. Differential Scanning Calorimetry

Our results thus far have demonstrated that intercalation occurs in many polymer:fullerene blends and that an interaction between the polymer and the fullerene cage is responsible for intercalation. Here, we probe this interaction using differential scanning calorimetry (DSC). The DSC heating curves for pure PBTTT-C14, pure PCBM-C70, and an intercalating PBTTT-C14:PCBM-C70 blend are shown **Figure 7**A. Figure 7B shows the corresponding DSC curves for the non-intercalated PBTTT-C14:BisPCBM-C70 material system.

The DSC scan for the intercalated PBTTT-C14:PCBM-C70 blend is very different than the DSC scans of pure PBTTT-C14 and pure PCBM-C70. A polymer:fullerene weight ratio of 40:60 (1:1 monomer:fullerene molar ratio) was chosen for the PBTTT-C14:PCBM-C70 blend, because 40:60 is the stoichiometry of the pure PBTTT-C14:PCBM-C70 bimolecular crystal without measureable excess PBTTT-C14 or PCBM-C70.[21] The DSC for this intercalated blend contains neither a peak due to PBTTT-C14 side-chain melting (~135 °C) nor a PCBM-C70 crystallization peak (the exothermic peak near 200 °C), since the blend film contains neither pure PBTTT-C14 nor pure PCBM-C70. Furthermore, the measured enthalpy associated with the backbone melting peak at ~225 °C is significantly larger in the blend (10.7 ± 0.8 J/g) than in the pure polymer (6.0 ± 0.6 J/g) due to the extra heat needed to overcome the interactions between the PBTTT-C14 and the PCBM-C70. Thus, these DSC scans give us

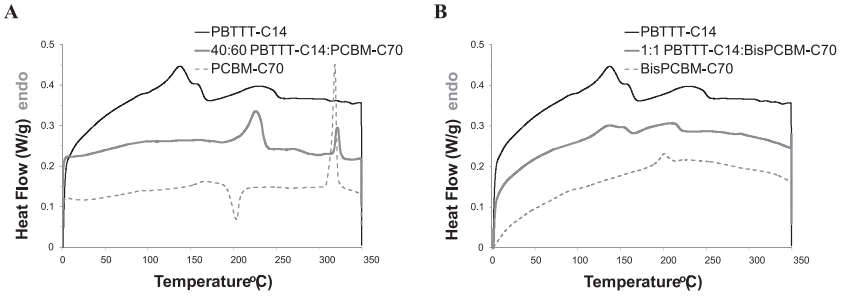


**Figure 7.** DSC heating scans for the intercalating PBTTT-C14:PCBM-C70 (A) and the non-intercalating PBTTT-C14:BisPCBM-C70 (B) material systems. The scans for the pure PBTTT-C14, pure fullerene and PBTTT-C14:fullerene blends are represented by the thin black line, the dashed grey line, and the thick grey line, respectively.

a measure of the strength of the polymer–fullerene interaction responsible for the thermodynamic stability of the intercalated PBTTT-C14:PCBM-C70 bimolecular crystal.

On the other hand, the DSC scan for the non-intercalated PBTTT-C14:BisPCBM-C70 blend (Figure 7B) contains contributions from both the pure PBTTT-C14 and pure BisPCBM-C70 and can be reconstructed fairly accurately by superimposing the DSC scans of the two pure components. In addition, there is no significant difference between the enthalpy of melting of the polymer in the pure PBTTT-C14 and PBTTT-C14:BisPCBM-C60 samples. These results confirm that there is little interaction between the components of the PBTTT-C14:BisPCBM-C70 blend, as would be expected for non-intercalating blends.

### 2.7. Molecular Simulations

We have carried out a series of molecular mechanics and molecular dynamics simulations on the crystalline structures of PBTTT-C14, PCBM-C70, adamantane, the PBTTT-C14:PCBM-C70 blend, and an hypothetical PBTTT-C14:adamantane blend. Our goal is to evaluate, at least qualitatively: (i) whether the polymer:molecule components are expected to mix, based on the calculation of the cohesive energy densities; and (ii) the strength of their interactions.

The model crystal structures of PBTTT-C14[55] and PBTTT-C14:PCBM-C70[21] were taken from previous work, and the crystal structure of adamantane was taken from the literature.[56] As there is no reported crystal structure for PCBM-C70, two possible structures were examined, based on the most stable crystalline forms of PCBM-C60 as determined by periodic density functional theory calculations:[57] a simple cubic structure (sc) and a triclinic structure that was generated by optimizing the sc structure (both with and without optimization of the unit cell). Here, we use the results for the triclinic unit cell since it was found to be the most energetically stable configuration. For the hypothetical blend of PBTTT-C14:adamantane, we considered a bimolecular structure analogous to that of the PBTTT-C14:PCBM-C70 crystal. Thus, uncertainties in our results come from the uncertainties in the determination of the PCBM-C70 and PBTTT-C14:adamantane crystals; this will prevent us from making quantitative assessments. The theoretical results reported below do point, however, to consistent trends with the experimental data.

To determine the cohesive energy densities of the pristine materials, we performed molecular dynamics simulations making use of the Universal force field (UFF).[58] Super cells of the three pristine systems (4 chains of a PBTTT-C14 pentamer, 20 PCBM-C70 molecules, and 96 adamantane molecules) were considered. The systems were equilibrated in the NVT ensemble at 300 K for 10–30 ps. This was followed by an NPT simulation at 300 K for 250 ps. The structures over the last 50 ps from the NPT run were collected and averaged to calculate the cohesive energy density of each system. The results show that PBTTT-C14 (636 J/cm$^3$) and PCBM-C70 (644 J/cm$^3$) have very similar cohesive energy densities, while that of adamantane (828 J/cm$^3$) is considerably larger. These cohesive energy densities translate into Hildebrand solubility parameters ($\delta$)[59–61] of 12.3 (cal/cm$^3$)$^{1/2}$ for PBTTT-C14, 12.4 (cal/cm$^3$)$^{1/2}$ for PCBM-C70, and 14.1 (cal/cm$^3$)$^{1/2}$ for adamantane. The similarity of the calculated data for PBTTT-C14 and PCBM-C70 underlines that the two systems should readily mix, while the substantial differences between the polymer and adamantane point to phase separation.[62]

We then gauged the total binding/intermolecular interaction energy within the blends by using the following equation:

$$E_{\text{binding}} = E_{\text{pol-mol}} - 2E_{\text{pol}} - 2E_{\text{mol}} \quad (1)$$

where $E_{\text{pol-mol}}$ is the unit-cell energy of the intercalated structure (bimolecular crystal) containing the polymer (pol) and the molecule (mol), and $E_{\text{pol}}$ and $E_{\text{mol}}$ represent the energy of the *isolated* components *pol* and *mol*, respectively. Note that $E_{\text{pol}}$ and $E_{\text{mol}}$ are multiplied by two as each molecule and polymer appears twice in the intercalated-blend unit cell. In this way, $-E_{\text{binding}}$ can be seen as corresponding to the enthalpy of sublimation of the bimolecular crystal. The energies entering Equation (1) were evaluated at the molecular mechanics level with the UFF.

The results demonstrate that the binding energy for the PBTTT-C14:PCBM-C70 crystal, –1448 kJ/mol per unit cell, is much larger than for the (hypothetical) PBTTT-C14:adamantane crystal, –1022 kJ/mol per unit cell. The driving force for the intercalation of PCBM-C70 amongst the PBTTT-C14 side chains appears to be mainly associated with van der Waals interactions (as opposed to electrostatic interactions). We note however that ground-state charge transfer, which might occur to some limited extent in these systems, is not considered explicitly in the present simulations. Quantum-mechanical calculations are currently being carried out to evaluate such processes. In any event, the theoretical results are in agreement with the experimental data and indicate that van der Waals interactions play a strong role in the formation and stabilization of the intercalated PBTTT-C14:PCBM-C70 structure.

## 3. Conclusion

Our investigations reveal several important factors that can affect the intercalation of fullerenes and small molecules between the side chains of conjugated polymers. First, fullerene intercalation does not occur if the fullerene cannot fit between the polymer side chains. Thus, fullerene intercalation can be inhibited by increasing the fullerene size by the addition of multiple bulky side groups or by decreasing the space available between the polymer side chains for fullerene intercalation, either by decreasing the side-chain repeat distance or by replacing linear side chains with bulkier, branched side chains. Although many conjugated and non-conjugated small molecules do not form polymer:fullerene bimolecular crystals, F4-TCNQ, a strong small-molecule acceptor, intercalates in PBTTT-C14 and is expected to form a ground-state charge-transfer complex with PBTTT-C14. While a ground-state charge-transfer complex could also form to some extent in polymer:fullerene bimolecular crystals, the molecular simulations indicate that van der Waals interactions alone are large enough to stabilize fullerene intercalation. The results obtained in this work provide a solid framework in which to understand why polymers and fullerenes molecularly mix in many bulk heterojunction solar cells and afford a basis in which to control molecular mixing so as to rationally design new, high-efficiency solar cells.

## 4. Experimental Section

*Materials*: PBTTT-C12, -C14, and -C16 were synthesized as described in reference.[25] PBTTT-Branched was synthesized in analogy to the previous reference. The number average molecular masses ($M_n$) of PBTTT-C12, -C14, -C16, and -Branched were determined to be 28, 22, 35, and 13 kDa with polydispersities of 1.8, 2.0, 2.0, and 1.6, respectively, using gel permeation chromatography against polystyrene standards. PCBM-C60 and PCBM-C70 was purchased from NanoC, BisPCBM-C70 was purchased from Solenne, and PQT was purchased from American Dye Source. C60, PCBM-C84, adamantane, TCNQ, F4-TCNQ, pyrene, coronene, and Kelevan were purchased from Sigma-Aldrich. ICMA-C60, ICBA-C60, and ICTA-C60 were provided by Plextronics. The remaining diamoindoids, V-BT, LuPCBEH-C80, and the dihydronaphthyl-bridged ester fullerene derivatives were synthesized as described in references,[63,64,26] and,[27] respectively. The vinyl functionalized SSQ precursor to SSQ-Es was purchased from Hybrid Plastics, Inc. The octavinylsilsesquioxane (OVS) was purchased from Mayaterials, Inc. Palladium catalyzed Heck chemistry was used to couple methyl 3-bromobenzoate to the vinyl functionalized SSQ precursor.[65]

*X-ray Diffraction*: Films for the XRD measurements were spin cast from ortho-dichlorobenzene (DCB) onto silicon substrates, slow dried in a covered petrii dish, and annealed at 180 °C for 10 minutes. Because C60 is not sufficiently soluble in DCB due to its lack of a solubilizing side group, PBTTT:C60 films were formed by evaporating C60 on top of a pure PBTTT-C14 film and annealing at 125 °C for 10 minutes. Specular XRD and 2D GIXS measurements were performed at X-ray energies of 8 keV and 12.735 keV on beamlines 2-1[13] and 11-3[12] at the Stanford Synchrotron Radiation Lightsource, respectively.

*Differential Scanning Calorimetry*: Samples for DSC were prepared by drop casting from DCB solutions onto clean glass substrates. The dried films were scraped off the substrates with a razor blade and placed in hermetically sealed pans. The samples were measured in flowing nitrogen according to the procedure described in reference 20 using a TA Instruments Q100 DSC with heating and cooling rates of 10 °C/min.

## Supporting Information

Supporting Information is available from the Wiley Online Library or from the author.

## Acknowledgements

This work was supported by the Center for Advanced Molecular Photovoltaics (Award No KUS-C1-015-21), made by King Abdullah University of Science and Technology (KAUST). Work at Georgia Tech was also supported by the Office of Naval Research (N00014-11-1-0211). The authors would like to acknowledge Darin Laird of Plextronics and Jeremy E.P. Dahl for the synthesis and purification of the indene-C60 fullerenes and the diamondoids, respectively. We would also like to acknowledge D.F. Kavulak and Jean M.J. Fréchet of the University of California in Berkeley and Martin Drees of Luna Innoations for the synthesis of the dihydronaphthyl bridged ester fullerene derivatives and the LUPCBEH-C80, respectively. Portions of this research were carried out at the Stanford Synchrotron Radiation Lightsource, a national user facility operated by Stanford University on behalf of the US Department of Energy, Office of Basic Energy Sciences. We acknowledge the permission to use the diffraction image processing and data analysis software package *Wxdiff* by Stefan C.B. Mannsfeld at SSRL (http://code.google.com/p/wxdiff).

Received: June 1, 2012
Revised: June 27, 2012
Published online: August 22, 2012

[1] G. Yu, J. Gao, J. C. Hummelen, F. Wudl, A. J. Heeger, *Science* **1995**, *270*, 1789.
[2] C. J. Brabec, S. Gowrisanker, J. J. M. Halls, D. Laird, S. Jia, S. P. Williams, *Adv. Mater.* **2010**, *22*, 3839.
[3] A. J. Moulé, K. Meerholz, *Adv. Funct. Mater.* **2009**, *19*, 3028.
[4] W. Yin, M. Dadmun, *ACS Nano* **2011**, *5*, 4756.
[5] D. Chen, A. Nakahara, D. Wei, D. Nordlund, T. P. Russell, *Nano Lett.* **2011**, *11*, 561.
[6] B. A. Collins, E. Gann, L. Guignard, X. He, C. R. McNeill, H. Ade, *J. Phys. Chem. Lett.* **2010**, *1*, 3160.
[7] N. D. Treat, M. A. Brady, G. Smith, M. F. Toney, E. J. Kramer, C. J. Hawker, M. L. Chabinyc, *Adv. Energy Mater.* **2011**, *1*, 82.
[8] D. R. Kozub, K. Vakhshouri, L. M. Orme, C. Wang, A. Hexemer, E. D. Gomez, *Macromolecules* **2011**, *44*, 5722.
[9] M. Pfannmöller, H. Flügge, G. Benner, I. Wacker, C. Sommer, M. Hanselmann, S. Schmale, H. Schmidt, F. A. Hamprecht, T. Rabe, W. Kowalsky, R. R. Schröder, *Nano Lett.* **2011**, *11*, 3099.
[10] C. Müller, J. Bergqvist, K. Vandewal, K. Tvingstedt, A. S. Anselmo, R. Magnusson, M. I. Alonso, E. Moons, H. Arwin, M. Campoy-Quiles, O. Inganas, *J. Mater. Chem.* **2011**, *21*, 10676.
[11] N. C. Cates, R. Gysel, J. E. P. Dahl, A. Sellinger, M. D. McGehee, *Chem. Mater.* **2010**, *22*, 3543.
[12] A. C. Mayer, M. F. Toney, S. R. Scully, J. Rivnay, C. J. Brabec, M. Scharber, M. Koppe, M. Heeney, I. McCulloch, M. D. McGehee, *Adv. Funct. Mater.* **2009**, *19*, 1173.
[13] N. C. Cates, R. Gysel, Z. Beiley, C. E. Miller, M. F. Toney, M. Heeney, I. McCulloch, M. D. McGehee, *Nano Lett.* **2009**, *9*, 4153.
[14] W. L. Rance, A. J. Ferguson, T. McCarthy-Ward, M. Heeney, D. S. Ginley, D. C. Olson, G. Rumbles, N. Kopidakis, *ACS Nano* **2011**, *5*, 5635.
[15] T. J. Savenije, W. J. Grzegorczyk, M. Heeney, S. Tierney, I. McCulloch, L. D. A. Siebbeles, *J. Phys. Chem. C* **2010**, *114*, 15116.
[16] A. Baumann, T. J. Savenije, D. H. K. Murthy, M. Heeney, V. Dyakonov, C. Deibel, *Adv. Funct. Mater.* **2011**, *21*, 1687.
[17] J. K. J. van Duren, X. Yang, J. Loos, C. W. T. Bulle-Liewma, A. B. Sieval, J. C. Hummelen, R. A. J. Janssen, *Adv. Funct. Mater.* **2004**, *14*, 425.
[18] V. D. Mihailetchi, L. J. A. Koster, P. W. M. Blom, C. Melzer, B. de Boer, J. K. J. van Duren, R. A. J. Janssen, *Adv. Funct. Mater.* **2005**, *15*, 795.
[19] T. Martens, J. D'Haen, T. Munters, Z. Beelen, L. Goris, J. Manca, M. D'Olieslaeger, D. Vanderzande, L. De Schepper, R. Andriessen, *Synth. Met.* **2003**, *138*, 243.
[20] N. C. Miller, R. Gysel, C. E. Miller, E. Verploegen, Z. Beiley, M. Heeney, I. McCulloch, Z. Bao, M. F. Toney, M. D. McGehee, *J. Polym. Sci., Part B: Polym. Phys.* **2011**, *49*, 499.
[21] N. C. Miller, E. Cho, M. J. N. Junk, R. Gysel, C. Risko, D. Kim, S. Sweetnam, C. E. Miller, L. J. Richter, R. J. Kline, M. Heeney, I. McCulloch, A. Ammassian, D. Acevedo-Feliz, C. Knox, M. R. Hansen, D. Dudenko, B. E. Chmelka, M. F. Toney, J.-L. Brédas, M. D. McGehee, *Adv. Mater.* **2012**, DOI: adma.201202293.
[22] F. C. Jamieson, E. B. Domingo, T. McCarthy-Ward, M. Heeney, N. Stingelin, J. R. Durrant, *Chem. Sci.* **2012**,*3*, 485.
[23] N. Banerji, S. Cowan, M. Leclerc, E. Vauthey, A. J. Heeger, *J. Am. Chem. Soc.* **2010**, *132*, 17459.
[24] C. Bruner, N. C. Miller, M. D. McGehee, R. Dauskardt, Unpuplished.
[25] I. McCulloch, M. Heeney, C. Bailey, K. Genevicius, I. Macdonald, M. Shkunov, D. Sparrowe, S. Tierney, R. Wagner, W. M. Zhang, M. L. Chabinyc, R. J. Kline, M. D. McGehee, M. F. Toney, *Nat. Mater.* **2006**, *5*, 328.
[26] R. B. Ross, C. M. Cardona, D. M. Guldi, S. G. Sankaranarayanan, M. O. Reese, N. Kopidakis, J. Peet, B. Walker, G. C. Bazan, E. Van Keuren, B. C. Holloway, M. Drees, *Nat. Mater.* **2009**, *8*, 208.
[27] S. A. Backer, K. Sivula, D. F. Kavulak, J. M. J. Fréchet, *Chem. Mater.* **2007**, *19*, 2927.

[28] N. C. Miller, S. Sweetnam, E. T. Hoke, R. Gysel, C. E. Miller, J. A. Bartelt, X. Xie, M. F. Toney, M. D. McGehee, *Nano Lett.* **2012**.
[29] M. S. Dresselhaus, G. Dresselhaus, P. C. Eklund, *Science of Fullerenes and Carbon Nanotubes*, Academic Press, Inc., San Diego **1996**.
[30] R. J. Kline, D. M. DeLongchamp, D. A. Fischer, E. K. Lin, L. J. Richter, M. L. Chabinyc, M. F. Toney, M. Heeney, I. McCulloch, *Macromolecules* **2007**, *40*, 7960.
[31] Z. E. Ooi, T. L. Tam, R. Y. C. Shin, Z. K. Chen, T. Kietzke, A. Sellinger, M. Baumgarten, K. Mullen, J. C. de Mello, *J. Mater. Chem.* **2008**, *18*.
[32] C. H. Woo, T. W. Holcombe, D. A. Unruh, A. Sellinger, J. M. J. Fréchet, *Chem. Mater.* **2010**, *22*, 1673.
[33] P. Pingel, L. Zhu, K. S. Park, J.-O. Vogel, S. Janietz, E.-G. Kim, J. P. Rabe, J.-L. Brédas, N. Koch, *J. Phys. Chem. Lett.* **2010**, *1*, 2037.
[34] N. Koch, *Chem. Phys. Chem.* **2007**, *8*, 1438.
[35] L. Zhu, E.-G. Kim, Y. Yi, J.-L. Brédas, *Chem. Mater.* **2011**, *23*, 5149.
[36] K. Vandewal, K. Tvingstedt, A. Gadisa, O. Inganas, J. V. Manca, *Nat. Mater.* **2009**, *8*, 904.
[37] J. J. Benson-Smith, L. Goris, K. Vandewal, K. Haenen, J. V. Manca, D. Vanderzande, D. D. C. Bradley, J. Nelson, *Adv. Funct. Mater.* **2007**, *17*, 451.
[38] L. Goris, K. Haenen, M. Nesládek, P. Wagner, D. Vanderzande, L. Schepper, J. D'haen, L. Lutsen, J. Manca, *J. Mater. Sci.* **2005**, *40*, 1413.
[39] L. Goris, A. Poruba, L. Hod'akova, M. Vanecek, K. Haenen, M. Nesladek, P. Wagner, D. Vanderzande, L. D. Schepper, J. V. Manca, *Appl. Phys. Lett.* **2006**, *88*, 052113.
[40] C. Deibel, T. Strobel, V. Dyakonov, *Adv. Mater.* **2010**, *22*, 4097.
[41] J. E. Parmer, A. C. Mayer, B. E. Hardin, S. R. Scully, M. D. McGehee, M. Heeney, I. McCulloch, *Applied Physics Letters* **2008**, *92*, 113309.
[42] M. Koppe, M. Scharber, C. Brabec, W. Duffy, M. Heeney, I. McCulloch, *Adv. Funct. Mater.* **2007**, *17*, 1371.
[43] C.-H. Cho, H. Kang, T. E. Kang, H.-H. Cho, S. C. Yoon, M.-K. Jeon, B. J. Kim, *Chem. Commun.* **2011**, *47*, 3577.
[44] L. Biniek, S. Fall, C. L. Chochos, D. V. Anokhin, D. A. Ivanov, N. Leclerc, P. Lévêque, T. Heiser, *Macromolecules* **2010**, *43*, 9779.
[45] C. Piliego, T. W. Holcombe, J. D. Douglas, C. H. Woo, P. M. Beaujuge, J. M. J. Fréchet, *J. Am. Chem. Soc.* **2010**, *132*, 7595.
[46] H.-Y. Chen, J. Hou, S. Zhang, Y. Liang, G. Yang, Y. Yang, L. Yu, Y. Wu, G. Li, *Nat. Photon.* **2009**, *3*, 649.
[47] Y. Liang, Z. Xu, J. Xia, S.-T. Tsai, Y. Wu, G. Li, C. Ray, L. Yu, *Adv. Mater.* **2010**, *22*, E135.
[48] T.-Y. Chu, J. Lu, S. Beaupré, Y. Zhang, J.-R. m. Pouliot, S. Wakim, J. Zhou, M. Leclerc, Z. Li, J. Ding, Y. Tao, *J. Am. Chem. Soc.* **2011**, *133*, 4250.
[49] S. C. Price, A. C. Stuart, L. Yang, H. Zhou, W. You, *J. Am. Chem. Soc.* **2011**, *133*, 4625.
[50] H. J. Son, W. Wang, T. Xu, Y. Liang, Y. Wu, G. Li, L. Yu, *J. Am. Chem. Soc.* **2011**, *133*, 1885.
[51] I. McCulloch, M. Heeney, M. L. Chabinyc, D. DeLongchamp, R. J. Kline, M. Cölle, W. Duffy, D. Fischer, D. Gundlach, B. Hamadani, R. Hamilton, L. Richter, A. Salleo, M. Shkunov, D. Sparrowe, S. Tierney, W. Zhang, *Adv. Mater.* **2009**, *21*, 1091.
[52] A. J. Wise, M. R. Precit, A. M. Papp, J. K. Grey, *ACS Appl. Mater. Interfaces* **2011**, *3*, 3011.
[53] Z. M. Beiley, E. T. Hoke, R. Noriega, J. Dacuña, G. F. Burkhard, J. A. Bartelt, A. Salleo, M. F. Toney, M. D. McGehee, *Adv. Energy Mater.* **2011**, *1*, 954.
[54] M. R. Hammond, R. J. Kline, A. A. Herzing, L. J. Richter, D. S. Germack, H.-W. Ro, C. L. Soles, D. A. Fischer, T. Xu, L. Yu, M. F. Toney, D. M. DeLongchamp, *ACS Nano* **2011**.
[55] E. Cho, C. Risko, D. Kim, R. Gysel, N. C. Miller, D. W. Breiby, M. D. McGehee, M. F. Toney, R. J. Kline, J.-L. Brédas, *J. Am. Chem. Soc.* **2012**, *134*, 6177.
[56] J. Donohue, S. H. Goodman, *Acta Cryst.* **1967**, *22*, 352.
[57] J. M. Nápoles-Duarte, M. Reyes-Reyes, J. L. Ricardo-Chavez, R. Garibay-Alonso, R. López-Sandoval, *Phys. Rev. B* **2008**, *78*, 035425.
[58] A. K. Rappe, C. J. Casewit, K. S. Colwell, W. A. Goddard, W. M. Skiff, *J. Am. Chem. Soc.* **1992**, *114*, 10024.
[59] J. H. Hildebrand, R. L. Scott, *The Solubility of Non-Electrolytes*, Reinhold New York **1936**.
[60] A. R. Tiller, B. Gorella, *Polymer* **1994**, *35*, 3251.
[61] M. Belmares, M. Blanco, W. A. Goddard, R. B. Ross, G. Caldwell, S. H. Chou, J. Pham, P. M. Olofson, C. Thomas, *J. Comput. Chem.* **2004**, *25*, 1814.
[62] M. Rubenstein, R. H. Colby, *Polymer Physics*, Oxford University Press, New York **2003**.
[63] J. E. Dahl, S. G. Liu, R. M. K. Carlson, *Science* **2003**, *299*, 96.
[64] R. Y. C. Shin, P. Sonar, P. S. Siew, Z.-K. Chen, A. Sellinger, *J. Org. Chem.* **2009**, *74*, 3293.
[65] M. Y. Lo, C. Zhen, M. Lauters, G. E. Jabbour, A. Sellinger, *J. Am. Chem. Soc.* **2007**, *129*, 5808.